

See discussions, stats, and author profiles for this publication at: <https://www.researchgate.net/publication/354724631>

Cine-MRI Simulation to Evaluate Tumor Tracking

Chapter · September 2021

DOI: 10.1007/978-3-030-87592-3_13

CITATIONS

0

READS

48

6 authors, including:



José D. Tascón-Vidarte
University of Copenhagen

12 PUBLICATIONS 5 CITATIONS

[SEE PROFILE](#)



Isak Wahlstedt
Technical University of Denmark

22 PUBLICATIONS 53 CITATIONS

[SEE PROFILE](#)



Kenny Erleben
University of Copenhagen

86 PUBLICATIONS 955 CITATIONS

[SEE PROFILE](#)



Sune Darkner
University of Copenhagen

87 PUBLICATIONS 528 CITATIONS

[SEE PROFILE](#)

Some of the authors of this publication are also working on these related projects:



Rainbow [View project](#)



Modeling and Solving Friction Force Problems [View project](#)



Cine-MRI Simulation to Evaluate Tumor Tracking

José D. Tascón-Vidarte^{1(✉)}, Isak Wahlstedt^{2,3}, Julien Jomier⁴,
Kenny Erleben¹, Ivan R. Vogelius², and Sune Darkner¹

¹ Department of Computer Science, University of Copenhagen,
Copenhagen, Denmark

{jota,kenny,darkner}@di.ku.dk

² Department of Oncology, Rigshospitalet, Copenhagen, Denmark

{isak.hannes.wahlstedt,ivan.richter.vogelius}@regionh.dk

³ Technical University of Denmark, Kongens Lyngby, Denmark

⁴ Kitware SAS, Villeurbanne, France

julien.jomier@kitware.com

Abstract. Conventional evaluations of tumor tracking algorithms require inter-observer segmentations from radiation oncologists on the Cine-MRI (2D sagittal MR video). Instead of performing intensive manual annotations on images, we present a 2D video simulator that uses the pre-treatment images, including a breathing model, that generates Cine-MR images in parallel with the underlined segmentation of the tumor. We include the data of seven patients within a retrospective clinical study that received stereotactic body radiation therapy for liver metastases. Each patient has a pre-treatment 4DCT scan, a pre-treatment 3D MR with tumor and liver delineations, and the treatment Cine-MRI. We augment the data with the simulator by changing breathing motion parameters and adding noise. The simulator generates a total of 84 Cine-MRI sequences, thus having 12 videos per patient. We validate the simulated versus the real Cine-MRI in terms of tumor motion. Finally, we used the simulator to evaluate the performance of real-time tumor tracking algorithms with this dataset.

Keywords: Cine-MRI · Simulation · Tumor tracking · Real-time · Image-guided radiotherapy

1 Introduction

An MR-linac is a device that combines magnetic resonance imaging with a linear accelerator. Stereotactic body radiotherapy (SBRT) of liver metastases on the MR-Linac system is advantageous due to the improved soft-tissue contrast compared to cone-beam computed tomography [12]. In addition, the MR-Linac has beam gating, i.e. the treatment accelerator beam is triggered in response to patient movement [4]. The clinical advantages of using an MR-linac with online

tracking have been demonstrated [1], indicating the potential to reduce the liver target volume and lower the radiation dose to adjacent organs at risk.

Liver tumors deform and move during treatment mainly caused by breathing motion [14]. During treatment, the scanner acquires 2D cine-MR sagittal images at four (4) frames per second [16]. Tumor tracking is one of the main components of beam gating in the MR-Linac system. Tumor tracking is solved automatically using image analysis. Some proposed strategies for tumor tracking are based on template matching [3, 19], feature detection [15], optical-flow methods [17, 23], deformable image registration [5], segmentation [9], neural networks [22] or modeling based [8]. The difficulty in evaluating tumor tracking is the need for ground truth data as no publicly available datasets that comprise tumor tracking on Cine-MRI exist. This requires manually delineation of the tumor in the entire video by a radiation oncologist [3, 5, 19, 22]. Evaluations are therefore only comparable at the institutional level. A generalized methodology to easily evaluate tumor tracking is required.

In addition, current tracking systems used in clinical practice may fail to track unexpected movements and have difficulty in tracking motion in the out-of-plane direction [16]. The breath-hold treatment is the most used respiratory motion management in practice [6]. After breath-hold, the patients can exhibit a fast motion, and thus tracking becomes very difficult. All the previously reported studies evaluate tumor tracking under free-breathing conditions [3, 5, 8, 15, 17, 19, 22, 23]. Thus, there is a need for improved tracking algorithms under varying breathing motion.

Our contribution is a straightforward evaluation methodology to quantify tumor tracking performance without the need of manual segmentations. The method is patient-specific and simple to implement. We demonstrate the capabilities of our method to create multiple simulated Cine-MRI, and to evaluate tumor tracking algorithms under varying conditions.

2 Related Work

Respiratory motion modeling is an extensively studied field [13]. Deformable image registration generates the most suitable models [20]. Likewise, our breathing model works with deformable image registration. Fu et al. [7] use known deformation fields to create ground truth images and landmarks to validate feature detection on 4DCT. Our simulator works in a similar way, but in contrast the known transformation model is applied to the images and the tumor contours.

The use of pre-treatment 4D imaging data has been exploited for treatment. Harris et al. [11] use 4DMRI to create synthetic 4DCT during treatment on conventional linear accelerators. Garau et al. [8] use pre-treatment 4DCT with treatment Cine-MRI to estimate a 3DCT and compare planning versus treatment. The mentioned methods suggest multi-modal integration of images and that pre-treatment time-sequence images are valid to model breathing motion during treatment. We aim for a similar goal with a distinction, to build a breathing model based on registration, use the model to simulate treatment sequences,

in order to improve tumor tracking algorithms. To our knowledge this is the first Cine-MRI simulation based on a respiratory motion model.

An alternative option to manually delineate the tumor is to use matched landmarks [15, 17]. Although this process can be automated with feature detection algorithms some outliers occur. Furthermore, the landmark distance alone does not represent how well the tracking algorithm performs with respect to the tumor structure and the contours. Most tumor tracking algorithms have been tested on lung patients with manual delineations of the tumor [3, 5, 19, 22] and only a small set has been evaluated on liver patients with landmarks [15, 17]. We test the proposed methodology and the tracking algorithms with liver patients. Identifying a tumor contour on a sagittal slice is difficult in the liver due to the lack of contrast. Hence, the liver is a remarkable example of why manual tumor delineations for evaluating tumor tracking are not always feasible.

3 Methods

3.1 Data

This study uses image data from seven patients already treated with SBRT for metastases in the liver at Rigshospitalet (Copenhagen, Denmark) between April and December 2019. The patients provided informed consent and approval for the usage of their anonymized data for research purposes.

Respiratory correlated 4DCT with intravenous contrast injection was performed for all patients on a SOMATOM Definition AS scanner (Siemens Healthineers, Germany). 4DCT image data were phase-sorted into ten phase bins throughout a respiratory cycle based on an external respiratory signal monitored with Real-Time Position Management (RPM, Varian Medical Systems, USA). The slice separation in each phase of the 4DCT was 2 mm. The image resolution in each slice was 512×512 pixels and a pixel size of 0.98×0.98 mm.

A 0.3T MRIDIAN MR-Linac (ViewRay, USA) is used to acquire a pre-treatment 3D MRI and the Cine-MRI sequences. The 3D MR scans were performed for all patients in inspiration breath-hold position without visual guidance. The acquisition technique is balanced steady-state free precession (bSSFP). The pre-treatment image resolution is $[512 \times 512 \times 128 \text{ pixels}]$ and $[1.5 \times 1.5 \times 3.0 \text{ mm}]$ spacing. The Cine-MRI sequences (bSSFP-Sagittal) have a resolution of $[256 \times 256 \text{ pixels}]$ and $[1.5 \times 1.5 \text{ mm}]$ spacing. The clinical gross tumor volume was delineated on the 3D MR by a senior radiologist and approved by a senior oncologist. Organs at risk, including the liver, were also delineated. These delineated contours are used to segment the region of interest (ROI).

3.2 Cine-MRI Simulation

We developed a patient-specific Cine-MRI simulator capable to generate a simulated ground truth contour of the desired organs using pre-treatment images. The input images are a 4DCT scan and an MR with organ contours. The video

simulator has the following input parameters: video time, frames per second, breathing cycle time, breathing amplitude, and additive noise. Figure 1 illustrates the video simulation process. Algorithm 1 details the simulator pseudo code. The simulator has two stages: breathing modeling and video synthesis. Each stage is described in the following.

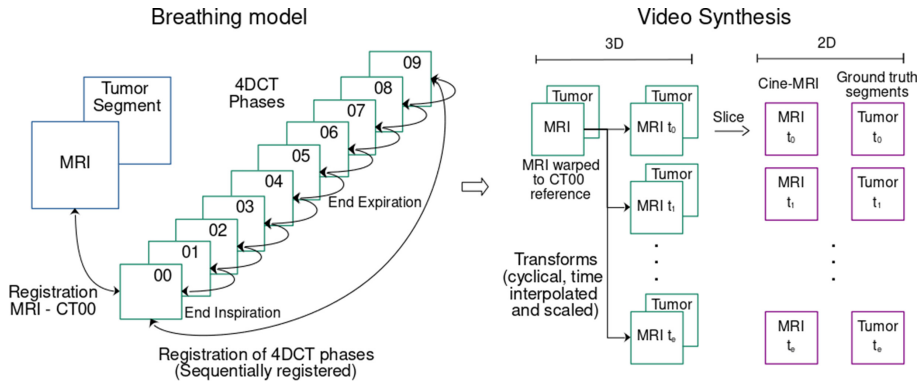


Fig. 1. 2D Cine-MRI Simulator. The process comprises two stages: breathing modeling and video synthesis. The breathing model is a pre-processing stage and uses full 3D information to consider out-of-plane motion in the 2D Cine-MRI. The video synthesis stage can be run several times changing the simulation parameters to create different variants and motion conditions.

The breathing modeling is a pre-processing stage. It is computed once and stored in order to create several videos. This model is based on the 4DCT scan that represents the full respiratory cycle of each patient. Initially, all phases in the 4DCT are registered sequentially with the symmetric normalization algorithm [2]. Subsequently, the MR image is registered to phase 00 of the 4DCT scan, since both images are at inspiration position. This transformed MR is the starting video frame.

The video synthesis stage is an iterative stage. The simulator produces a new video frame as a composition of sequential transformations related to the 4DCT. The corresponding transformation is interpolated over time to match the proportion of the respiratory cycle with the video sample time. The video is created based on 3D images and transformations. From this a 2D slice is extracted in the sagittal view where the tumor has better visibility. Thus the simulated video has the same complexity as real 3D motion in the 2D images and simulates the MR-Linac imaging setup, where 2D real-time images are acquired and tracked. Since the initial contour of the tumor and organs are known in the reference MR, we create independent files with those regions of interest (ROI) and the ROI are transformed in parallel with the raw video image generation. For simplicity we only generate the tumor contours. Therefore, we have the ground truth ROI for each video sample.

Algorithm 1. Cine-MRI Simulation

Input: 4DCT, 3D MRI (bSSFP) and clinical tumor contour**Parameters:** Video time, frames per second, breathing cycle time, breathing amplitude, and additive noise**Output:** Cine-MRI (Video containing 2D bSSFP-Sagittal images)

- 1: Register sequentially 4DCT images, and store transformations
 $\varphi_{00 \rightarrow 01}, \varphi_{01 \rightarrow 02}, \dots, \varphi_{09 \rightarrow 00}$ where $j = 00, 01, \dots, 09$ correspond to the phase;
 - 2: Register MRI image to 4DCT phase 00 obtain $\varphi_{MR \rightarrow 00}$;
 - 3: Transform MRI image to CT phase 00 using $\varphi_{MR \rightarrow 00}$, obtain M_{00} ;
 - 4: Transform tumor delineation X_{MR} using $\varphi_{MR \rightarrow 00}$ to get contour X_{00} ;
 - 5: Compute simulation *time* using parameters: video time, frames per second;
 - 6: **for** t in *time* **do**
 - 7: Compute time point t location in breathing cycle;
 - 8: Calculate time proportion for time interpolation t_δ ;
 - 9: Find the shortest path of sequential transformations;
 - 10: Compose a transformation $\varphi_c(x)$ with the shortest path;
 - 11: Multiply $\varphi_c(x)$ with breathing amplitude parameter α ;
 - 12: Transform image M_{00} using $\varphi_c(x)$, obtain M_t ;
 - 13: Extract a slice of M_t to create the image $M_{2d,t}$;
 - 14: Add noise to image $M_{2d,t}$;
 - 15: Transform contour X_{00} using $\varphi_c(x)$, obtain X_t ;
 - 16: Extract a slice of X_t to create the image $X_{2d,t}$;
 - 17: **end for**
-

The simulator supports noise with two different probability distributions: Gaussian and Rician distributions. Noise in MR images is often modeled as Rician, and for signal to noise ratio greater than two, the noise behaves like Gaussian [10]. Furthermore, other sources of noise from the MR device are still modelled as Gaussian.

3.3 Tracking Algorithms

The MR-Linac typical rate of acquisition is four (4) frames per second [16]. Tracking algorithms must meet this time requirement. The first image and its corresponding tumor contour in the Cine-MR sequence is used as the reference and the tracking algorithms uses the subsequent Cine-MRI input images to estimate a new tumor contour. Fast et al. [5] presented a comparative study where they analyzed four tumor tracking techniques. The authors concluded that all the algorithms had a relatively similar performance but among them deformable image registration and template matching provided slightly better results. We implemented these two algorithms to evaluate tumor tracking simulator. Both algorithms are implemented on C++ and parallelized on CPU with OpenMP.

We chose the diffeomorphic demons [21] as a fast solution of deformable image registration. Our approach uses a multiresolution framework with three pyramidal levels. The computational bottleneck of registration is the computation of

the transformation and the similarity metric [18]. We focused on this stage to improve performance. Regarding the optimization, we fix the iteration values to be able to achieve the time restriction, this means that full convergence is not always guaranteed.

We implemented the generalized template matching algorithms [3, 19]. The algorithm defines a template in a reference image, usually the tumor bounding box, and search for it in a local region of the input image by maximizing an objective function to determine a good match. The preferred function is cross-correlation for Cine-MR tracking. The wider the search region is, the more computational time, while with a more limited search region, there is a risk of not capturing the tumor motion.

3.4 Metrics

We used three metrics to validate the real and simulated Cine-MRI and to evaluate the tumor tracking algorithms. First, the Dice Similarity Coefficient, which serves to quantify the whole segmented structure. Secondly, the centroid distance, which quantify the algorithm’s ability to follow the center of mass (COM) of the tumor. And third, the Hausdorff distance, which provides a measurement of the effectiveness to detect and track the tumor contours. Further information regarding the metrics are detailed in Fast et al. [5].

4 Experiments and Results

4.1 Patient Summary

Table 1 summarizes the patients tumor and breathing motion. The patient set is small in numbers but represents a wide variety of anatomical tumor location, tumor size, breathing motion, and breathing cycle times. The most challenging conditions for the tracking algorithms are a short tumor displacement or a small tumor area.

Table 1. Summary of patient information. Tumor location is the geometric octant of where the tumor is with regards to the liver center of mass. The abbreviations correspond to Superior-Inferior, Anterior-Posterior, and Left-Right. Breathing cycle times were determined from real patient respiratory motion during 4DCT scans. Tumor displacements refer to the maximum motion presented in the video without registration. Gross tumor volumes/areas are estimated on the reference 3D/2D (sagittal) MR.

Patient	1	2	3	4	5	6	7
Tumor location (geometric)	S-A-L	S-A-L	S-A-R	I-A-L	S-A-R	S-P-L	I-P-R
Breathing cycle (mean) [s]	4.8	3	4.1	3.6	4.4	4.1	5.8
Tumor max. displacement [mm]	5.9	9.1	8.1	9.7	2.0	6.5	12.6
Tumor volume [cm^3]	5.5	5.6	12.0	3.1	3.1	8.0	5.7
Tumor sagittal area [cm^2]	2.7	3.0	7.4	3.3	1.8	4.7	4.1

4.2 Cine-MRI Image Quality

Figure 2 shows a comparison between the real Cine-MRI and the simulation for one patient. All the resulting videos are visually close to the real Cine-MRI. To validate the real versus the simulated Cine-MRI, we verify how consistent the tumor motion is for all the patients. We select 12 images (approximately a breathing cycle) of the real Cine-MRI with the first image in the inspiration position. The tumors are segmented manually on the real Cine-MRI. Since the real and the simulated data have a slightly different field of view, we perform rigid registration around the tumor on the first image and align the remaining simulation images using the same transformation. We calculate the metrics for all the patients with the real versus the simulated Cine-MRI. The Dice score is 0.89 ± 0.05 (*mean* \pm *std.dev.*), the centroid distance 0.78 ± 0.32 mm and Hausdorff distance 2.11 ± 0.91 mm.

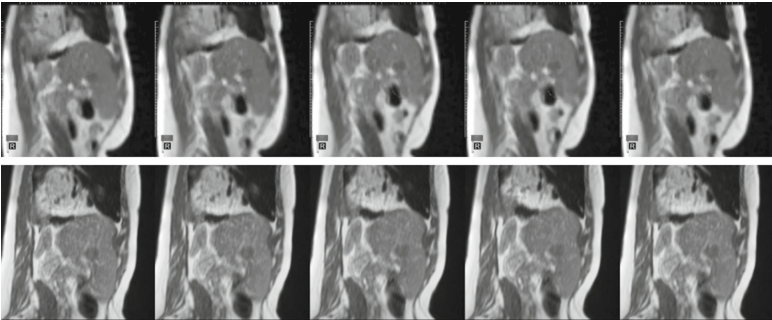


Fig. 2. Video comparison of real Cine-MRI and simulated of one patient. Top images depict the real Cine-MRI and the bottom images the simulation.

4.3 Tumor Tracking Performance

We evaluate tumor tracking with a full factorial experiment between breathing amplitude and noise. The breathing amplitude is varied with values 1.0, 1.5, 2.0, or random. The noise is varied between none, Gaussian and Rician. Gaussian noise and Rician noise applied in all the tests are equivalent to 20% of added noise. These experiments generate 12 videos per patient for a total of 84 Cine-MRI sequences. The breathing cycle parameter is patient-specific taken from Table 1. All the videos are 20s long at 4 frames per second (80 images), approximately 4–5 breathing cycles.

Figure 3 depict the tumor tracking performance. For comparison, we compute a baseline (in blue) that corresponds to the metric value without tracking. Videos 1 to 4 vary in amplitude without noise, videos 5 to 8 vary in amplitude with Gaussian noise, and videos 9 to 12 vary in amplitude with Rician noise. Video 1 is the most representative as it has the default and control conditions. The

Dice score summary as *mean* \pm *standarddeviation* results of registration are 0.88 ± 0.06 , template matching 0.79 ± 0.12 . The centroid distance obtained for the registration is 0.89 ± 0.54 mm versus template matching 1.71 ± 3.81 mm. The Hausdorff distance obtained for registration is 3.23 ± 1.35 mm versus template matching 4.41 ± 4.02 mm. Both algorithms' performance in terms of centroid distances is adequate for image-guided radiotherapy.

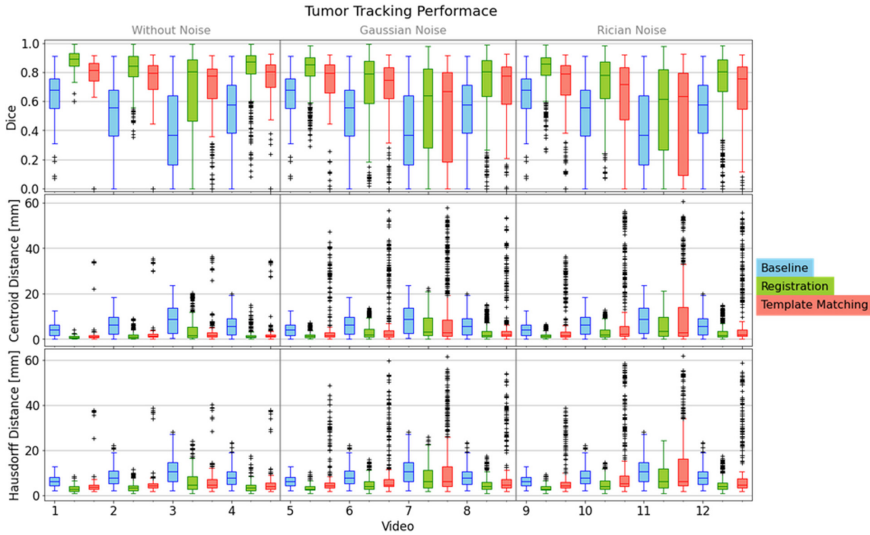


Fig. 3. Video statistics of tumor tracking. The metrics are estimated per video and comprise all patients. Videos are generated as a full factorial experiment between breathing amplitude and added noise. Ascending numbers in groups of 4 videos correspond to breathing amplitude of 1, 1.5, 2, and random respectively. The metrics are shown from top to bottom as Dice, centroid distance, and Hausdorff distance. In blue, the baseline as the metrics computed without tracking. In green, the metrics determined with registration. In red, the metrics estimated with template matching. (Color figure online)

All the tests were run on a workstation with 2 CPUs and 128 GB of RAM. Each CPU is an Intel(R) Xeon(R) Silver 4110 @ 2.10 GHz, 8 cores, 16 threads. The computational time of the deformable registration algorithm time is on average 62.7 ms with a standard deviation of 42.3 ms. The maximum registration time is 242 ms. The computational time of the template matching algorithm is on average 16.7 ms with a standard deviation of 4.4 ms.

5 Discussion and Conclusion

We validate the tumor motion between the real versus the simulated Cine-MRI. The centroid distance is the best metric to represent the motion, and its mean

value distance of 0.78 mm indicates a high similarity between the real and the simulated data. We do not compare image intensities between the real and the simulated Cine-MRI because they come from sources acquired on different dates and under different conditions (pre-treatment - treatment, the field of view, alignment, among others). Furthermore, a direct comparison of pixel intensities or image similarity will only reveal how close they are in terms of signal, contrast, or even alignment but not how well the simulation model breathing and tumor motion.

Regarding our specific evaluation of tumor tracking algorithms, we identify in general that deformable image registration perform better. The template matching algorithm fails under noisy conditions and present several outliers. A breathing amplitude of 2.0 is an extreme condition and unrealistic. However, from the algorithms point of view is an interesting experiment. Both tracking algorithms fails to follow the tumor having wide ranges of Dice scores under this condition.

A limitation of our Cine-MRI simulator is that the breathing model uses a single respiratory cycle from the 4DCT scan. The breathing model overcomes this by composing transformations that are time interpolated. Time interpolation guarantees that different patterns arise due to asynchrony between the patient's breathing cycle time and sampling times. Furthermore, when we model with full 3D images and then create the 2D Saggital MR, we incorporate the desired out-of-plane motion, which is the main challenge for tracking algorithms. Overall, our goal is not to create a perfect breathing model but to facilitate challenging experiments to evaluate tumor tracking algorithms.

We designed a platform and a methodology to easily evaluate tracking algorithms on Cine-MR with ground truth segmentation. The video simulator does not require any training data and works only with pre-treatment images. The proposed methodology is the most automated way to evaluate tumor tracking algorithms with a ground truth. Our code is open source and available at <https://github.com/josetascon/cinemri-simulation>.

Acknowledgment. This project has received funding from the European Union's Horizon 2020 research and innovation program under the Marie Skłodowska-Curie grant agreement No. 764644. This paper only contains the author's views and the Research Executive Agency and the Commission are not responsible for any use that may be made of the information it contains.

References

1. Al-Ward, S., et al.: The radiobiological impact of motion tracking of liver, pancreas and kidney SBRT tumors in a MR-linac. *Phys. Med. Biol.* **63**(21), 215022 (2018)
2. Avants, B.B., Epstein, C.L., Grossman, M., Gee, J.C.: Symmetric diffeomorphic image registration with cross-correlation: evaluating automated labeling of elderly and neurodegenerative brain. *Med. Image Anal.* **12**(1), 26–41 (2008)
3. Cervino, L.I., Du, J., Jiang, S.B.: MRI-guided tumor tracking in lung cancer radiotherapy. *Phys. Med. Biol.* **56**(13), 3773 (2011)

4. Crijs, S., Kok, J., Lagendijk, J., Raaymakers, B.: Towards MRI-guided linear accelerator control: gating on an MRI accelerator. *Phys. Med. Biol.* **56**(15), 4815 (2011)
5. Fast, M.F., et al.: Tumour auto-contouring on 2d cine MRI for locally advanced lung cancer: a comparative study. *Radiother. Oncol.* **125**(3), 485–491 (2017)
6. Feldman, A.M., Modh, A., Glide-Hurst, C., Chetty, I.J., Movsas, B.: Real-time magnetic resonance-guided liver stereotactic body radiation therapy: an institutional report using a magnetic resonance-linac system. *Cureus*, **11**(9) (2019)
7. Fu, Y., Wu, X., Thomas, A.M., Li, H.H., Yang, D.: Automatic large quantity landmark pairs detection in 4dct lung images. *Med. Phys.* **46**(10), 4490–4501 (2019)
8. Garau, N., et al.: A ROI-based global motion model established on 4DCT and 2D cine-MRI data for MRI-guidance in radiation therapy. *Phys. Med. Biol.* **64**(4), 045002 (2019)
9. Gou, S., Wu, J., Liu, F., Lee, P., Rapacchi, S., Hu, P., Sheng, K.: Feasibility of automated pancreas segmentation based on dynamic MRI. *Br. J. Radiol.* **87**(1044), 20140248 (2014)
10. Gudbjartsson, H., Patz, S.: The Rician distribution of noisy MRI data. *Magn. Reson. Med.* **34**(6), 910–914 (1995)
11. Harris, W., Wang, C., Yin, F.F., Cai, J., Ren, L.: A novel method to generate on-board 4D MRI using prior 4D MRI and on-board KV projections from a conventional linac for target localization in liver SBRT. *Med. Phys.* **45**(7), 3238–3245 (2018)
12. Kontaxis, C., Bol, G., Stemkens, B., Glitzner, M., Prins, F., Kerkmeijer, L., Lagendijk, J., Raaymakers, B.: Towards fast online intrafraction replanning for free-breathing stereotactic body radiation therapy with the MR-linac. *Phys. Med. Biol.* **62**(18), 7233 (2017)
13. McClelland, J.R., Hawkes, D.J., Schaeffter, T., King, A.P.: Respiratory motion models: a review. *Med. Image Anal.* **17**(1), 19–42 (2013)
14. Murphy, M.J.: Tracking moving organs in real time. In: *Seminars in Radiation Oncology*, vol. 14, pp. 91–100. Elsevier (2004)
15. Paganelli, C., et al.: Magnetic resonance imaging-guided versus surrogate-based motion tracking in liver radiation therapy: a prospective comparative study. *Int. J. Radiat. Oncol*. Biol*. Phys.* **91**(4), 840–848 (2015)
16. Paganelli, C., et al.: MRI-guidance for motion management in external beam radiotherapy: current status and future challenges. *Phys. Med. Biol.* **63**(22), 22TR03 (2018)
17. Seregini, M., Paganelli, C., Summers, P., Bellomi, M., Baroni, G., Riboldi, M.: A hybrid image registration and matching framework for real-time motion tracking in MRI-guided radiotherapy. *IEEE Trans. Biomed. Eng.* **65**(1), 131–139 (2017)
18. Shams, R., Sadeghi, P., Kennedy, R.A., Hartley, R.I.: A survey of medical image registration on multicore and the GPU. *IEEE Signal Process. Mag.* **27**(2), 50–60 (2010)
19. Shi, X., Diwanji, T., Mooney, K.E., Lin, J., Feigenberg, S., D’Souza, W.D., Mistry, N.N.: Evaluation of template matching for tumor motion management with cine-MR images in lung cancer patients. *Med. Phys.* **41**(5), 052304 (2014)
20. Stemkens, B., Tijssen, R.H., De Senneville, B.D., Lagendijk, J.J., Van Den Berg, C.A.: Image-driven, model-based 3d abdominal motion estimation for MR-guided radiotherapy. *Phys. Med. Biol.* **61**(14), 5335 (2016)
21. Vercauteren, T., Pennec, X., Perchant, A., Ayache, N.: Diffeomorphic demons: efficient non-parametric image registration. *Neuroimage* **45**(1), S61–S72 (2009)

22. Yun, J., Yip, E., Gabos, Z., Wachowicz, K., Rathee, S., Fallone, B.: Neural-network based autocontouring algorithm for intrafractional lung-tumor tracking using linac-MR. *Med. Phys.* **42**(5), 2296–2310 (2015)
23. Zachiu, C., Papadakis, N., Ries, M., Moonen, C., De Senneville, B.D.: An improved optical flow tracking technique for real-time MR-guided beam therapies in moving organs. *Phys. Med. Biol.* **60**(23), 9003 (2015)